M. Shane Hutson
George Holzwarth*
Department of Physics
Wake Forest University
Winston-Salem, North Carolina
27109-7507 USA

Thomas Duke
Departments of Physics and
Molecular Biology
Princeton University
Princeton, New Jersey
08544-0708 USA

Jean-Louis Viovy
Groupe de Physico-Chimie
Théorique (URA CNRS 1382)
Ecole Supérieure de Physique
et de Chimie Industrielles
de Paris
10 rue Vauquelin
75231 Paris Cedex 05, France

Two-Dimensional Motion of DNA Bands During 120° Pulsed-Field Gel Electrophoresis. I. Effect of Molecular Weight

The instantaneous position and velocity of bands of linear, double-stranded DNA were measured during 120° pulsed-field electrophoresis in 1% agarose gels, using a video micrometer capable of simultaneous measurements in two dimensions. When the direction of the field was switched, the band initially retraced the last portion of its path during the preceding pulse. The distance the band moved backward increased with DNA length: 48.5 kb (kilobase pair) DNA moved backward only 0.2 μm, but 1110 kb DNA moved backward 24 μm before setting off in a positive direction. The velocity of the DNA band was particularly rapid during the backward movement; the magnitude of the velocity spike increased with M, *reaching 2.4 μm/s for 1110 kb DNA, which was about 5 times the steady-state velocity. The velocity in the* y *direction, perpendicular to the mean drift direction, showed an even larger transient spike, which also increased with* M.

Simulation of the dynamics of long DNA chains undergoing gel electrophoresis by a dynamic Monte Carlo method gave instantaneous xy *position and velocity in excellent agreement with experiment. The simulation included extensional motions of the DNA within the tube of interconnected agarose pores as well as the possibility of loops (hernias) that escape laterally from the tube.* © *1995 John Wiley & Sons, Inc.*

Received May 24, 1994; accepted August 1, 1994.

* To whom correspondence should be addressed at Wake Forest University, P.O. Box 7507, Reynolda Station, Winston-Salem, NC 27109.

Biopolymers, Vol. 35, 297–306 (1995)

CCC 0006-3525/95/030297-10

INTRODUCTION

Pulsed-field gel electrophoresis (PFGE) is widely used to separate DNAs containing 50–5000 kb (kilobase pairs), but our understanding of the underlying molecular processes is still far from complete.[1–6] One reason is that the only experimental outcome reported in most PFGE studies is the net displacement of DNA bands after many cycles of changes in field direction. Unfortunately, the net displacement integrates out all details of the path traveled by the band on the way to its final destination and gives a deceptive simplicity to a complicated, time-dependent, two-dimensional process.

We have constructed a video micrometer that directly measures the two-dimensional path and instantaneous velocity of a band of fluorescently tagged DNA *while the PFGE field switches direction.*[7] The data obtained can test competing models of PFGE in more stringent ways than can mobility curves. In a previous paper, the effect of pulse period T on the path and velocity was reported for a single value of M and 120° field angle.[8] It was found that two analytic models—the constant velocity, flexible rod model of Southern and the biased reptation model without fluctuations—gave a poor fit to the measured velocity curves. Here, we extend this earlier experimental work by measuring the effect of DNA size M on the xy path and instantaneous velocity under typical 120° PFGE conditions. A parallel study on the effect of field angle is presented in the subsequent paper.[9]

Computer simulations that permit longitudinal fluctuations of the chain in the confining tube of gel constraints, as well as leakage (hernias) of the chain from the tube, have recently achieved considerable success in modeling the net band displacement and alignment during PFGE.[10–15] Rather than compare our new measurements to older theoretical models with demonstrated shortcomings, the experimentalists among the present authors (MSH and GH) initiated a collaboration with the other authors (TD and JLV) to test whether their model,[14,15] a nonlocal Monte Carlo simulation that permits longitudinal fluctuations as well as tube leakage, could fit the new data more successfully. The results of this confrontation between new data and a current model are included in the present report.

The field directions and (x, y) coordinate system used in describing the results of both experiment and simulation are shown in Figure 1. In this figure, the vectors QE_A and QE_B show the direction of the electric force on the DNA during alternate pulses; θ is the angle between QE_A and QE_B, 120° in these experiments. The mean drift direction of the DNA is along the bisector of QE_A and QE_B; this is chosen as the x axis.

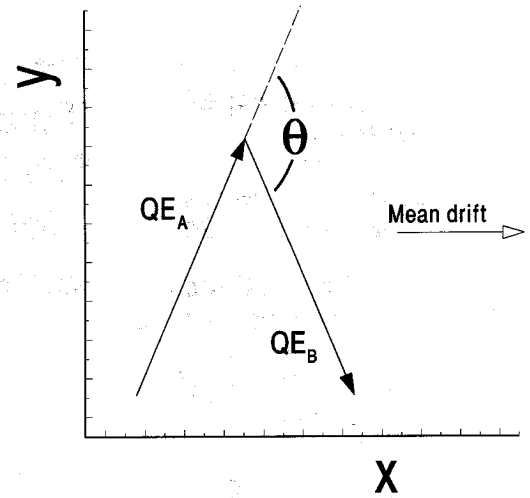

FIGURE 1 Coordinate system for the experiments. The electric force is directed alternately along directions QE_A and QE_B, with $|E_A| = |E_B|$. The angle θ between QE_A and QE_B is equal to 120°. The duration of QE_A or QE_B is T. The xy coordinate system used to describe the motions of a band is oriented so that x is parallel to the mean drift direction of the DNA.

MATERIALS AND METHODS

DNA, Gels, Buffer

Buffer was 0.5 × TBE (45 mmol Tris base, 45 mmol boric acid, 1.25 mmol EDTA, pH 8.3). Gels were prepared with filtered 1% agarose having endosmosis 0.10–0.15 (FMC SeaKem LE), as previously described.[8]

Four DNAs were used. (1) λ-DNA (48.5 kb) was purchased from Gibco BRL. (2) T4-DNA (170 kb) and (3) G-DNA (670 kb) were obtained from Carolina Biological Supply Co. as a suspension of the respective intact phages. The DNA was released from the phage by adding "SDS/ficoll/EDTA/dye mix,"[16] heating for 10 min at 65°C, then cooling to 0°C. The size of G-DNA was based upon its electrophoretic mobility relative to the chromosomes of *Saccharomyces cerevisiae.* (4) Yeast DNA (*S. cerevisiae* strain YPH80) in agarose beads was obtained from Gibco BRL (megabase I DNA standard). Chromosomes XV (1100 kb) and VII (1120 kb), separated as described below, were used for measurements.

A gel containing λ-, T4-, or G-DNA in a sharp band of undegraded molecular weight was prepared in a two-step procedure. First, the DNA was run into the gel with a 0.75 V/cm DC field for 30 min. This was followed by 4 h at 4 V/cm in a Bio-Rad CHEF II system with a pulse

ramp of 3–30, 9–15, or 100–300 s for the respective DNAs. Yeast DNA was eased into the gel at low voltage, as above, then subjected to 20 h of 120° CHEF electrophoresis with $T = 80$ s and $E = 4$ V/cm, followed by 10 h of 120° CHEF with $T = 120$ s. The gel containing λ-, T4-, G-, or yeast DNA was then stained with 0.1 μg/mL EB (ethidium bromide), destained in 0.5 × TBE, and photographed on a 300 nm transilluminator. Chromosomes XV and VII of yeast were identified from their mobilities.[17] The bands of DNA in each case retained the V shape of the wells without distortion as they drifted in the x direction.

Electrophoresis Chamber and Field Electronics

The chamber was constructed of clear polymethylmethacrylate. Buffer (14°C) was recirculated at 300 mL/min over the gel and through a chiller. Twenty-four platinum electrodes, arranged in a hexagon, were used to define the magnitude and direction of the two electric fields E_A and E_B in the gel. The potential at each electrode was clamped[18] by a prototype BioRad CHEF II-DR circuit board, generously provided by Charles Ragsdale of BioRad, to provide uniform fields E_A and E_B directed at 120° to one another. Measured potential maps showed that the field lines were straight and the angle between E_A and E_B was 118° ± 3° throughout the gel. Signals to switch between E_A and E_B were sent by a computer that also controlled image acquisition.

Video Micrometer

The position of a band of fluorescently labeled DNA in a gel was determined by illuminating the band through the bottom of the chamber with 50–200 mW of 488–514 nm light from an argon-ion laser and observing the fluorescent image of the band from above with a video camera, as described previously.[8] Images were digitized by a Matrox Image 1280 board operating in an 80386 microcomputer host. Band position in pixels was determined on the board in real time by an intensity-weighted centroid algorithm:

$$\langle i \rangle = \sum_{ij} iI_{ij} / \sum_{ij} I_{ij}$$

$$\langle j \rangle = \sum_{ij} jI_{ij} / \sum_{ij} I_{ij}$$

where i is the pixel column number, j is the pixel row number, and I_{ij} is the light intensity at that pixel. A precision of ±0.01 pixel was achieved over a period of 5 s; long-term precision was ±0.04 pixel. The relationship between band location $\langle i \rangle$, $\langle j \rangle$ in pixels at the camera and band position (x, y) in μm at the gel was controlled by the location and focal length of the camera lens. The conversion factors were determined by placing a steel scale at the object plane of the detector.[8]

The velocity components v_x and v_y were computed by differentiating $x(t)$ or $y(t)$ with respect to t, using the Savitzky-Golay 7-point first-derivative algorithm[19] provided in the AXUM software package (Trimetrix, Seattle, WA).

Simulations

Monte Carlo simulations were carried out as previously described.[14,15] The DNA chain was modeled as N segments, each corresponding to approximately 1 kb and carrying a charge q. The segments were connected by links that were either extended (taut), with length a, or contracted (relaxed), with length 0. The gel was represented by a three-dimensional network of interconnected pores with uniform center-to-center separation a; each pore could hold 1 or more segments. The electric force on each segment was incorporated through the reduced field strength, $\theta = qEa/kT$.

We have chosen parameters and conversion factors between simulation and experiment as follows: 1 segment = 1 kb; 1 time step = 10 ms; the length scale of the simulation, a, was set to 300 nm to approximate a 1% agarose gel, all consistent with physical measurements from a variety of sources, as previously explained.[14,15] The reduced field θ was set to 0.6, corresponding to $E = 4$ V/cm and charge $q = 135$ e^- per 1 kb segment. This value of q is 50% greater than we have used previously,[14,15] but remains within the bounds of uncertainty in the experimental measurement of this quantity, 0.08–0.2 e^-/bp. The value 0.135 e^-/bp was chosen so that simulation and experiment agree on both the steady-state velocity of a band and the resonant pulse time T^*. Other choices within the experimental range of q would not change the qualitative conclusions of this study. The instantaneous, two-dimensional position and velocity measurements newly reported here were not used in the selection of parameters for the simulation.

In contrast to earlier Monte Carlo simulations, the present version[14,15] permitted two novel processes. First, a slack segment was permitted to move to any point along an adjacent string of taut segments in a single step, rather than 1 segment at a time. Second, hernias were permitted if 2 or more slack segments occupied the same pore. Hernias are readily observed in video micrographs of DNA electrophoresis.[20–26] In the simulation, the predominant motion in steady fields changed from start-and-stop "inchworm dynamics,"[27] when $M < 200$ kb, to a more steady creation and retraction of one or more hernias or branches at constantly changing positions along the chain for larger M. The typical size of hernias was proportional to M, while the average number present at any instant increased only slowly (roughly logarithmically) with M. The resultant ramified structure of very long molecules can be thought of as a nested series of U- and J-shaped portions of the chain. The probability for hernia formation in the model was adjusted so as to fit the observed depth of the antiresonance mobility minimum in field-inversion gel electrophoresis.[15]

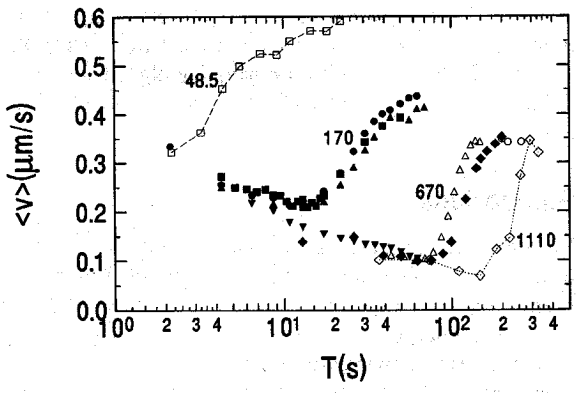

FIGURE 2 Average velocity during 120° PFGE of linear double-stranded DNA containing 48.5, 170, 670, and 1110 kb for a broad range of pulse durations T. □ 48.5 kb; ●, ■, and ▲ 170 kb; △, ◆, ▼, and ○ 670 kb; ◇ 1110 kb. Conditions: 1% LE agarose, 0.5 × TBE, 14°C, 4 V/cm.

RESULTS

Average Velocity

Before examining the dependence of instantaneous position and instantaneous velocity of DNA bands upon pulse duration T and molecular weight M, it is useful to orient oneself by considering how the *average* velocity $\langle v \rangle$ varies with T for a specific M; the average velocity is what is normally measured in a typical separation. Figure 2 shows $\langle v \rangle$ for pulse duration T between 2 and 300 s, with M = 48.5, 170, 670, and 1110 kb. As T decreased, $\langle v \rangle$ decreased to a minimum, often termed the antiresonance, at a time T^* characteristic of M, E, agarose concentration, etc. If we identify T^* with the mobility minimum, then T^* = 1.9, 13, 72, and 150 s for 48.5, 170, 670, and 1110 kb. From a study covering many more DNAs,[28] it was concluded that T^* varies as $M^{1.2}$. In our experiments, we have measured the center-of-mass path and velocity for T = 26, 76, and 200 s, corresponding to $(\frac{1}{3})T^*$, $T \approx T^*$, and $T \approx 3T^*$ for 670 kb.

Measured Center-of-Mass Path

The path followed by a band of DNA during a single cycle of 120° PFGE changed greatly as M increased (Figure 3). For T = 200 s, 48.5 kb DNA moved parallel to the changed direction of QE almost instantaneously, but 1110 kb DNA first essentially retraced a substantial portion of its path during the previous pulse, thus moving backward 24 μm in the $-x$ direction, opposite to the mean

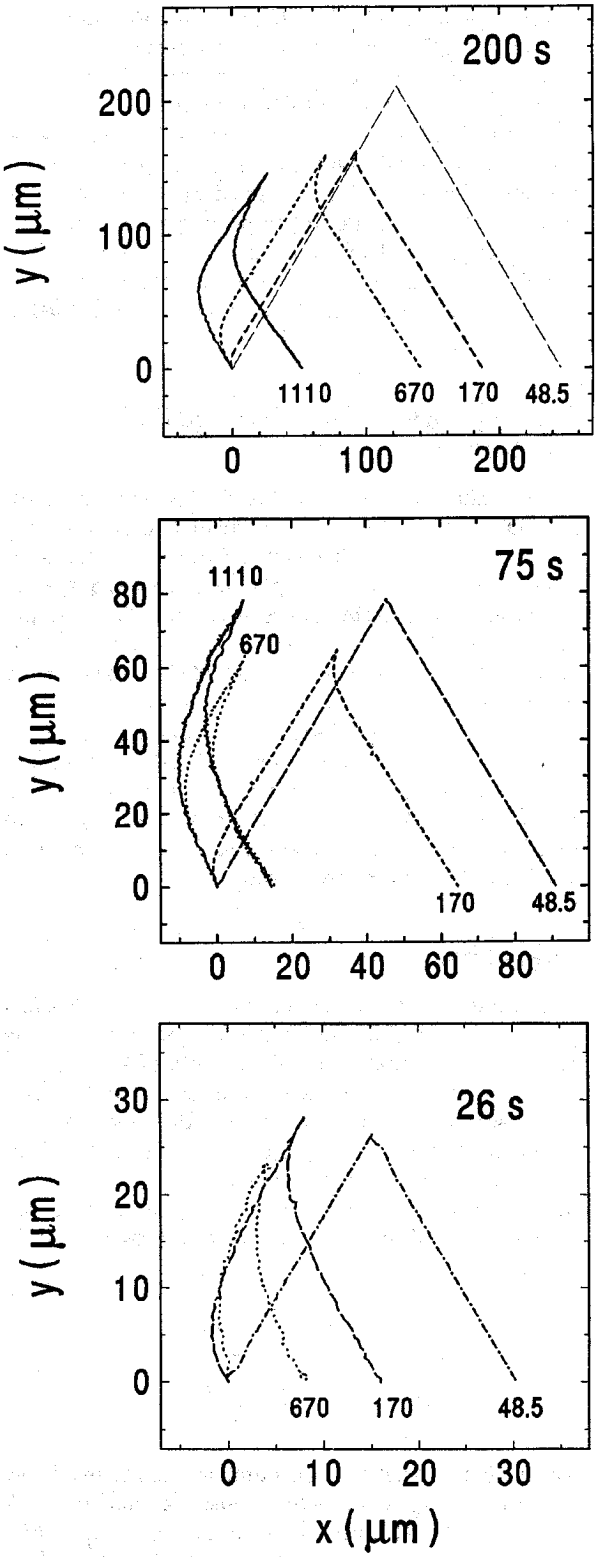

FIGURE 3 Experimentally determined position of a band of DNA during 1 complete cycle of 120° PFGE for DNA containing 48.5, 170, 670, and 1110 kb. Top: T = 200 s; middle: T = 75 s; bottom: T = 26 s. Conditions as in Figure 2.

drift direction. Because of the long time spent in this backward motion, the band barely had time to become aligned with QE before the field changed direction again. As a consequence, although the short DNA advanced 250 μm along the $+x$ direction during 400 s, the 1110 kb chains advanced only 55 μm. Intermediate Ms showed intermediate behavior. All four DNAs would have been well separated by a series of such 200 s pulses, but a single pulse would not have been sufficient, since bands typically have a width of 400–500 μm. The amplitude of motion in the y direction was similar for all chain lengths.

When T was shortened to 75 s, the xy paths changed, as shown in Figure 3 (middle panel). For 48.5 and 170 kb DNA, the path resembled the first 75 s of the path for 200 s. As a consequence, a larger *fraction* of the 75 s movement was spent in backward movement. A more dramatic change occurred for 670 kb DNA; this was expected because this value of T was close to T^* for this chain length (Figure 1). Backward movement so dominated the motion of both 670 and 1110 kb DNA that they advanced only 15 μm in the x direction while moving 65–80 μm from side to side. The field was on for such a short time that 1110 kb DNA never moved parallel to QE.

For T = 26 s, even 670 kb DNA did not have sufficient time to move parallel with the field (Figure 3, bottom). Nevertheless, the oscillations of the 670 kb band in the y direction, 23 μm, were proportionately just as large as those at 75 or 200 s, and the average drift velocity in the x direction, 0.15 μm/s, actually exceeded that at T = 75 s, 0.10 μm/s. A similar progression, in which an increasing fraction of each pulse was spent going backward, was also apparent in the behavior of 170 kb DNA (Figure 3).

Simulated Center-of-Mass Path

Figure 4 shows the simulated results for the same pulse durations and chain lengths used experimentally. For T = 200 s and 50 kb, the simulated chain moved in the direction QE almost continuously; the backward movement was negligible, as in the experiments. In the simulation of the 170 kb movement, the band retraced a small portion of its path in the previous pulse, as in the experiments; during most of the pulse, the DNA moved in the direction of QE. The net displacement in the x direction was 148 μm, slightly less than the experimental value, 190 μm. In the y direction the agreement was closer. As M increased to 670 and 1110 kb, both

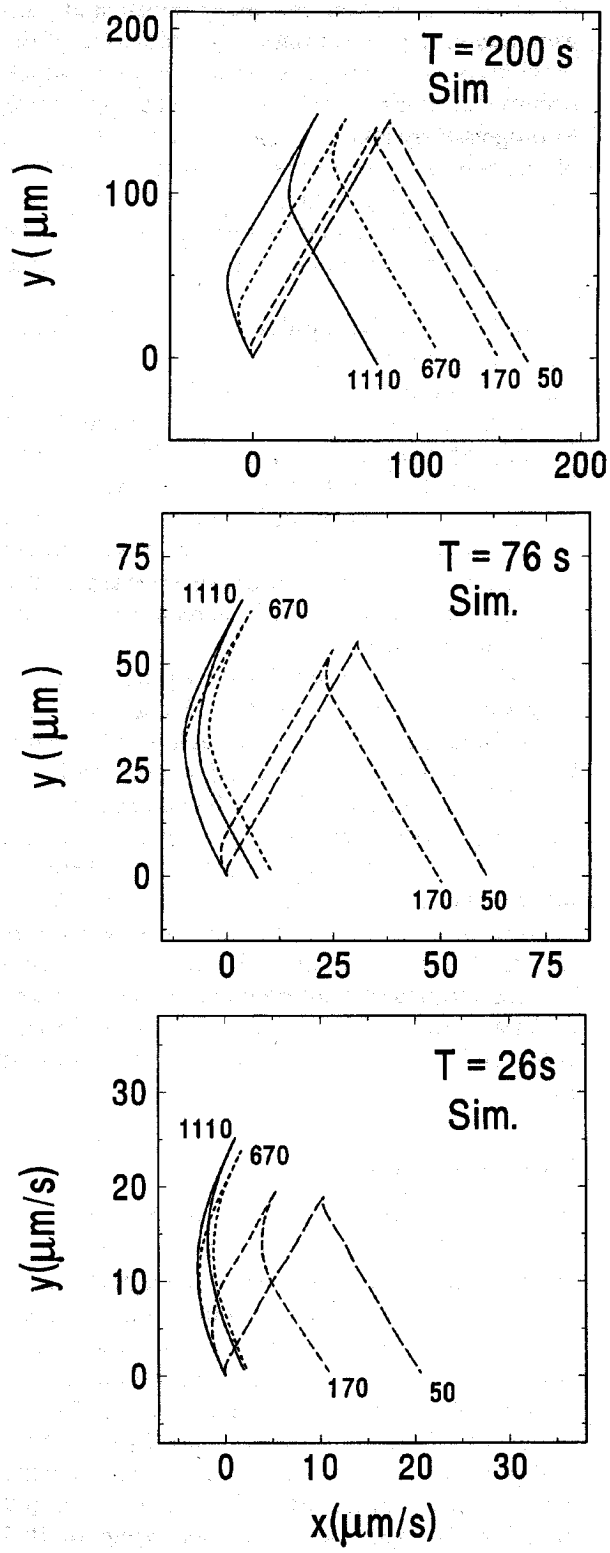

FIGURE 4 Simulated position of a band of DNA during 1 complete cycle of 120° PFGE for M = 50, 170, 670, and 1100 segments. Top: T = 200 s; middle: T = 76 s; bottom: T = 26 s. Reduced field = 0.6; 1 distance unit = 300 nm (1 pore); 1 time unit = 10 ms.

the simulated motion and the experimental path were increasingly dominated by a retracing of the previous path. The large backward motions, which occurred every time the field changed direction, led to progressively less net x displacement at the end of one complete cycle, reaching 76 μm at 1100 kb, compared to 50 μm in the experiments. Meanwhile, the amplitude of the simulated motion in the y direction was largely independent of M, as in the experiments.

For T = 76 s, the simulated xy motion changed only slightly for 50 and 170 kb, except that the displacements were less because the field was on for a shorter time. However, T = 76 s corresponds to T^* for 670 kb and the simulated 670 kb motion changed greatly from that at T = 200 s, with large y oscillations, large backward x motions, and net x displacement of only 11 μm per cycle (observed: 13 μm). For 1100 kb, the motions were almost the same as for 670 kb, again in agreement with the experimental results.

For T = 26 s, the simulated xy plots for 50 kb were similar to the observed results, although the net x displacement was somewhat less in the simulation. For 170 kb, simulated chains and real chains experienced a similar reduction in net x displacement while retaining large swings in the y direction. For 670 kb, the simulated net x displacement was only 2.2 μm while the y oscillations remained large, 25 μm; experimental behavior was similar (Figure 3, bottom). For this short T, neither the simulated chain nor experiment exhibited backward movements as large as those at 76 and 200 s, and the chains never moved parallel to E at any time.

Measured Velocity

The x vs y plots shown above provided a useful perspective on PFGE and a new test of the simulation, but they suppress the time dependence of the DNA motion contained in the original data. By differentiating x and y with respect to t, the x and y components of the velocity, v_x and v_y, were obtained. Figure 5 shows the experimental v_x and v_y for the same four values of M used in Figure 3, for T = 200 s. The most striking feature of the v_x data was the negative spike immediately after the field changed direction. The spike was barely detectable for 48.5 kb; however, for 1110 kb, its amplitude was 5 times the steady-state forward v_x and its duration ($v_x \leq 0$) was 33 ± 3 s. The corresponding v_y data (Figure 5, bottom) showed a large *positive* peak immediately after E changed direction, which also increased in

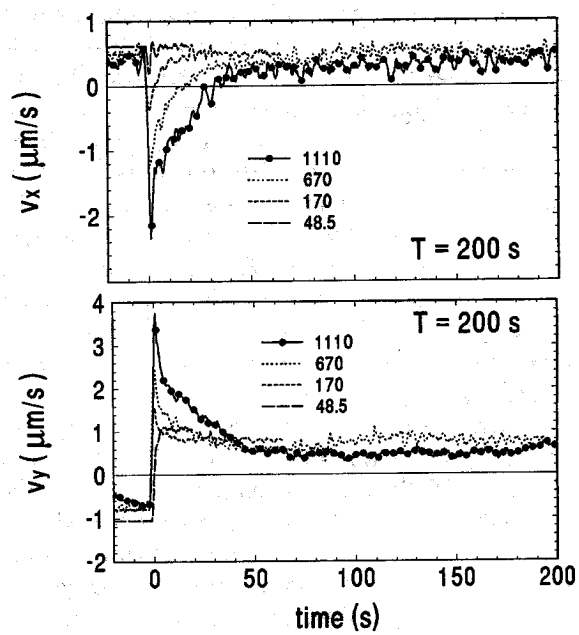

FIGURE 5 Experimentally determined velocity of a band of DNA during a single pulse of 120° PFGE with T = 200 s, for M = 48.5, 170, 670, and 1110 kb. Top: v_x; bottom: v_y. Other conditions as in Figure 2.

peak height and duration with larger M. The spike was followed by a shallow minimum followed in turn by a modest secondary peak, visible at 125 s for 670 kb DNA. The existence of this secondary peak demonstrates that the configurations of the roughly 10^8 molecules retained some correlation even 125 s after the time at which E last changed direction. Corresponding experimental velocity data for T = 75 and 26 s showed similar patterns,[29] but are not shown here.

Simulated Velocity

Differentiation of the simulated x and y data with respect to t yielded simulated v_x and v_y values, which for T = 200 s are shown in Figure 6. Comparison to the experimental curves (Figure 5) shows excellent agreement in the size, duration, and M dependence of the velocity spikes. The slightly larger amplitudes of the simulated peaks could easily originate in the finite time resolution of the experiments, 0.37 s.

The simulated v_y curves for T = 200 s are shown in Figure 6, bottom. Again, the amplitude and time duration were very similar to the experimental curves. Even the small secondary peak in v_y, which was experimentally observed near 125 s for 670 kb, appeared in the simulation.

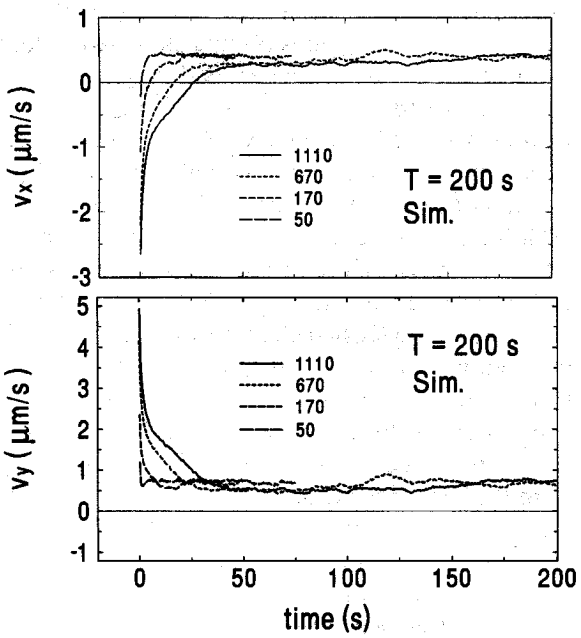

FIGURE 6 Simulated velocity of a band of DNA during a single pulse of 120° PFGE, for M = 50, 170, 670, and 1110 kb. Other conditions of the simulation were as in Figure 4.

DISCUSSION

The most important results are as follows:

1. The experimental demonstration that DNA bands spend a substantial portion of each pulse retracing the path created during the previous pulse, as first predicted by Southern.[30] The size of the backward displacements increases with increasing M; this is the dominant source of M dependence of the average mobility in 120° PFGE.
2. The finding that the velocity in the backward direction *increases* in both amplitude and duration as M increases, with backward velocities 7 times the steady-state v_x for 1110 kb DNA. This trend with M is counterintuitive, since the mobility *decreases* with increasing M.
3. The finding that the extended Monte Carlo simulation, which permits longitudinal fluctuations of the chain in the tube, as well as loops of the chain out of the tube,[14,15] with choices of parameter values that fall within bounds established by a variety of physical measurements, gives an accurate description not only of the *average* band velocity, which was known previously, but also of the xy path and the *instantaneous* velocity components v_x and v_y, which were not.

It is important to note two limitations of our experimental technique. First, all data are for EB-stained DNA. We have previously compared the mobility of DNA during 120° PFGE with and without EB, keeping the EB staining procedure similar to that used here. Under these conditions, EB causes the mobility to decrease by 10–15%.[31]

The second limitation of the experimental technique is time resolution. The band location was determined only every 0.37 s. When the field changed direction, the band velocity changed rapidly, within one data point, to the velocity peak. Thus, the peak heights we have determined are lower bounds.

In our first report of velocity measurements in two dimensions,[8] we showed that a band of G-DNA undergoing 120° PFGE exhibits large backward excursions each time the field changes directions. As T becomes shorter, but still keeping $T > T^*$, the amplitude of this backward motion changes little, but the band spends a progressively larger fraction of each pulse moving backward, thereby generating a mobility minimum at T = 75 s for E = 4 V/cm.

In the present article, it is shown that the amplitude of the backward motions increases as M increases. To get a better sense for the M dependence of the recoil amplitude, we have plotted the maximum backward distance against M; the results are shown in Figure 7. This varied from essentially 0 μm for 48.5 kb DNA to 24 μm for 1110 kb, for T = 200 s. The amplitude of the observed backward motion appeared to increase more steeply than

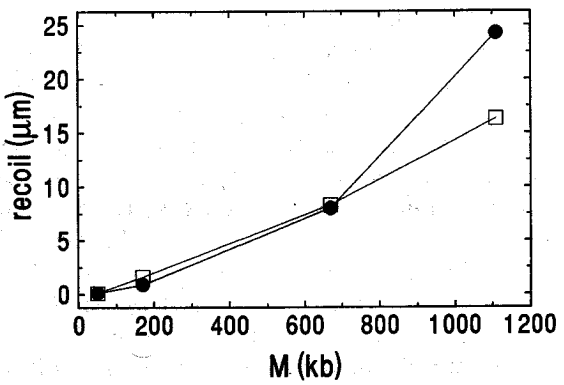

FIGURE 7 Dependence of the recoil distance in the x direction on chain length for T = 200 s. ●: Experimental recoil; □: simulated recoil.

M^1, although our data were too sparse to be certain of this.

The Monte Carlo simulation of the xy path behaved similarly to the experiments (Figure 4). For $T = 200$ s, the backward movements increased from 0.1 μm for 50 kb to 16 μm for $M = 1100$ kb (Figure 7). The differences between the simulated and experimental amplitudes are within the uncertainties in the appropriate reduced field and in the conversion between M and the number of segments in the simulated chain.

The qualitative explanation for the backward motion is apparent from video micrographs,[20–26] from measurements of the M dependence of the field-free recoil[7] and the alignment,[31–33] and from simulations.[10–15] These agree that DNA chains adopt highly extended configurations when they are driven by a field for a sufficient time in one direction. Video micrographs of fluorescently tagged DNA show highly elongated U, J, or herniated configurations, often with a bright spot, termed "bunching," at the leading end(s) of the chain. This bright spot is evidence that the local concentration of chain segments is elevated at the leading end(s) of the chain. Video micrographs show that the radius of gyration of the DNA chain increases dramatically, and fluctuates, as the chain is are driven through the gel.[24,26,34] Linear dichroism measurements show that the DNA helix axis becomes aligned in the field direction; the extent of alignment increases with increasing M.[32,33]

Backward motion of the band at the beginning of each pulse is easy to understand if each DNA chain is stretched out into a flexible rod of fixed length, which is a fraction of the contour length, as in Southern's model.[30] Southern suggested that the trailing end of the chain during one pulse becomes the leading end at the beginning of the next pulse. For short chains advancing by "inchworm dynamics,"[27] this can be true only in the sense of an averaged configuration; for chains in a U or J conformation, which are common in short chains, the trailing segments can be somewhere near the center of the chain in terms of the linear sequence. For larger M, however, both the MC simulation and video micrographs suggest that DNA chains are in ramified configurations with hernias. Although the exact size, position, and location of the hernias within a given chain, as well as the identity of the leading end, all fluctuate, the overall configuration of individual chains approximates a flexible rod of constant length.

Highly extended chain configurations have reduced entropy, which can be expressed in terms of intramolecular tension, as in the theory of rubber elasticity. Unlike the tension in a stretched rubber band or a symmetrically extended polymer chain, which causes the two ends to move in *opposite* directions toward the center when the ends are released, the tension in the U, J, and herniated configurations of DNA in a gel pulls the segments in both arms of the U or J in the *same* direction toward its base, causing a recoil. Measurements show that when E changes from 4 to 0 V/cm, the center of mass of the stretched chain recoils backward, on the average, about $\frac{1}{10}$th of the contour length of that DNA.[7] In 120° PFGE, both chain tension and a component of the electric force, $QE\sin(60)$, drive the stretched portions of the chain backward toward the base of the U or J, or toward the "trunk of the tree" in a ramified configuration. At the same time, in the simulation, segments from the bunched end move into the sequence of pores making up the stretched arms of the U or J. The velocity peak corresponds to the retraction of the arms of Us and hernias. This process continues until all the DNA has moved from the bunched end(s) to the base of the U or the originally trailing end of a herniated configuration. The subsequent shallow trough in v_y is due to the fact that there are then often a number of hernias competing to be the new head. Typically, they resolve into a slowly sliding U before the chain regains the standard constant-field behavior in the new direction of E.

This sequence of configurations is linked to the *distance* moved by the DNA, scaled by its molecular length L, after a change in field direction. The result is a transient partial synchronization of the motions of the 10^8 molecules in the band, giving the peak, trough, and secondary peak at times which scale with M. For 670 kb DNA, the measured minimum velocity occurs when the band has moved 60–65 μm along the xy path, which is $0.25L$ for this DNA. After the band has moved about 125 μm along the xy path, approximately $0.5L$, the secondary peak occurs. The distances moved are consistent with the simulated motion described in the preceding paragraph.

In Figures 5 and 6, it is apparent that the size of the velocity spike increases with M. In order to make this trend more quantitative, the amplitudes of the spikes in v_x and v_y were plotted against M for both experiment and simulation. The results are shown in Figure 8. The observed increase with M is captured quite accurately by the simulation, and both agree that the magnitude of the recoil increases as M increases. The simulated peaks may

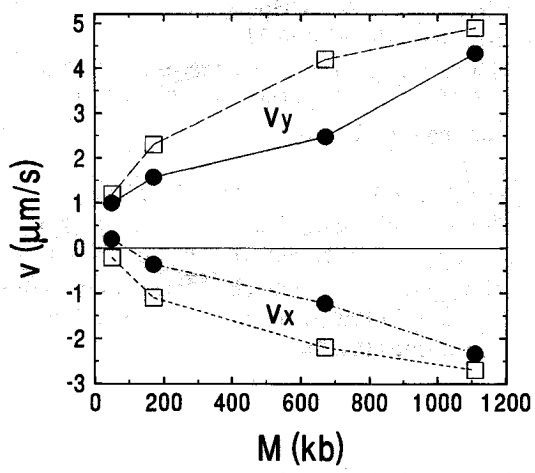

FIGURE 8 Dependence of peak velocity on molecular size. ●: Experimental results (data from Figure 5); □: simulated results (data from Figure 6). The top two curves show experimental and simulated v_y. The lower two curves show v_x.

be larger than the experimental peaks because of the finite time resolution of the experiments. Note that the peak velocities shown in this figure correspond to one value of T, 200 s. This particular value is greater than T^* for 48.5, 170, and 670 kb, but is near T^* for 1110 kb.

The increasing size of the velocity spike with increasing M in the simulation arises primarily from longer hops down the arms of the Us and back down the hernias, when the direction of the electric force changes. The longer hops down more extended sections of the chain correspond, physically, to a rate of elastic contraction that increases with the chain tension.

Extrapolation of the data in Figure 8 suggests what might happen if 120° PFGE were carried out under similar conditions for M = 10 Mb, the current upper limit of the technique. A band of 10 Mb DNA could experience peak v_x and $v_y \approx$ 15–25 μm/s, more than 20 times the steady-state values of v_x and v_y at 4 V/cm. Individual molecules might have even higher peak velocities. It is possible that the increasing recoil velocity with increasing M, or the increasing intramolecular chain tension that it reflects, are related to the trapping of DNA during PFGE, which becomes a problem as M and E increase.[35] The well-documented prevention of trapping through a reduction in E for larger M is consistent with this hypothesis.

MSH and GH are grateful for support by the National Science Foundation through grant DMB 8906213 and thank Louis Keiner and Lynn Neitzey for many helpful discussions. TD and JLV acknowledge support from the EEC Human Genome program.

REFERENCES

1. Viovy, J. L. & Defontaines, A. D. (1991) in *Pulsed-Field Gel Electrophoresis,* Burmeister, M. & Ulanovsky, L., Eds., Humana Press, Totawa, NJ, pp. 403–450.
2. Deutsch, J. M. (1991) in *Pulsed-Field Gel Electrophoresis,* Burmeister, M. & Ulanovsky, L., Eds., Humana Press, Totawa, NJ, pp. 367–384.
3. Nordén, B., Elvingson, C., Jonsson, M. & Åckerman, B. (1991) *Quart. Rev. Biophys.* **24,** 103–164.
4. Zimm, B. H. & Levene, S. D. (1992) *Quart. Rev. Biophys.* **25,** 171–204.
5. Viovy, J. L., Duke, T. & Caron, F. (1992) *Contemp. Phys.* **33,** 25–40.
6. Bustamante, C., Gurrieri, S. & Smith, S. B. (1993) *Trends Biotechnol.* **11,** 23–30.
7. Keiner, L. E. & Holzwarth, G. (1992) *J. Chem. Phys.* **97,** 4476–4484.
8. Neitzey, L. M., Hutson, M. S. & Holzwarth, G. (1993) *Electrophoresis* **14,** 296–303.
9. Neitzey, L. M., Holzwarth, G., Duke, T. & Viovy, J.-L. (1995) *Biopolymers* **35,** 307–317 accompanying article.
10. Lim, H. A., Slater, G. W. & Noolandi, J. (1990) *J. Chem. Phys.* **92,** 709–721.
11. Madden, T. L. & Deutsch, J. M. (1991) *J. Chem. Phys.* **95,** 1584–1591.
12. Zimm, B. H. (1991) *J. Chem. Phys.* **94,** 2187–2206.
13. Smith, S. B., Heller, C. & Bustamante, C. (1991) *Biochemistry* **30,** 5264–5274.
14. Duke, T. A. J. & Viovy, J. L. (1992) *Phys. Rev. Lett.* **68,** 542–545.
15. Duke, T. A. J. & Viovy, J. L. (1992) *J. Chem. Phys.* **96,** 8552–8563.
16. Carle, G. F., Frank, M. & Olson, M. V. (1986) *Science* **232,** 65–73.
17. Mathew, M. K., Smith, C. L. & Cantor, C. R. (1988) *Biochemistry* **27,** 9204–9210.
18. Chu, G., Vollrath, D. & Davis, R. W. (1986) *Science* **234,** 1582–1585.
19. Savitzky, A. & Golay, M. (1964) *Analyt. Chem.* **64,** 1627–1639.
20. Smith, S. B., Aldridge, P. K. & Callis, J. B. (1989) *Science* **243,** 203–206.
21. Smith, S. B. (1988) *Individual DNA Molecules Undergoing Gel Electrophoresis* (video tape), Instructional Media Services, SB-54, University of Washington, Seattle, WA 98195.
22. Schwartz, D. C. & Koval, M. (1989) *Nature* **338,** 520–522.
23. Gurrieri, S., Rizzarelli, E., Beack, D. & Bustamante, C. (1990) *Biochemistry* **29,** 3396–3401.

24. Rampino, N. J. (1991) *Biopolymers* **31,** 1009–1016.
25. Rampino, N. J. & Chrambach, A. (1991) *Biopolymers* **31,** 1297–1307.
26. Howard, T. & Holzwarth, G. (1992) *Biophys. J.* **63,** 1487–1492.
27. Deutsch, J. M. (1988) *Science* **240,** 922–928.
28. Chu, G. (1991) *Proc. Natl. Acad. Sci.* **88,** 11071–11075.
29. Hutson, M. S. (1993) Master's thesis, Department of Physics, Wake Forest University.
30. Southern, E. M., Anand, R., Brown, W. R. A. & Fletcher, D. S. (1987) *Nucleic Acids Res.* **15,** 5925–5943.
31. Whitcomb, R. W. & Holzwarth, G. (1991) *Nucleic Acids Res.* **18,** 6331–6337.
32. Holzwarth, G., McKee, C., Steiger, S. & Crater, G. (1987) *Nucleic Acids Res.* **15,** 10031–10044.
33. Åkerman, B. & Jonsson, M. (1990) *J. Chem. Phys.* **94,** 3828–3838.
34. Masubuchi, Y., Oana, H., Ono, K., Matsumoto, M., Doi, M., Minagawa, K., Matsuzawa, Y. & Yochikawa, K. (1993) *Macromolecules* **26,** 5269–5270.
35. Viovy, J.-L., Miomandre, F., Miquel, M.-C., Caron, F. & Sor, F. (1992) *Electrophoresis* **13,** 1–6, and references cited therein.